Side-Contact Representations with Convex Polygons in 3D: New Results for Complete Bipartite Graphs

André Schulz[0000−0002−2134−4852]

FernUniversität in Hagen, Universitätsstraße 47 58097 Hagen, Germany
andre.schulz@fernuni-hagen.de

Abstract. A polyhedral surface $\mathcal{C}$ in $\mathbb{R}^3$ with convex polygons as faces is a *side-contact representation* of a graph G if there is a bijection between the vertices of G and the faces of $\mathcal{C}$ such that the polygons of adjacent vertices are exactly the polygons sharing an entire common side in $\mathcal{C}$. We show that $K_{3,8}$ has a side-contact representation but $K_{3,250}$ has not. The latter result implies that the number of edges of a graph with side-contact representation and n vertices is bounded by $O(n^{5/3})$.

Keywords: Contact Representations · Polyhedral Surfaces · 3D.

1 Introduction

Contact representations are a classical approach to visualize graphs. A graph G has a contact representation if there is a bijection between its vertex set V and a set of interior-disjoint geometric objects from a given class such that two objects touch if and only if the corresponding vertices are adjacent. For a concrete contact representation it has to be specified, which geometric objects are considered (including their embedding space) and what it means for two objects to touch. In this paper we consider convex polygons in 3D as geometric objects. To avoid confusion we call the edges of a polygon its *sides* and the vertices its *corners*. Two polygons touch with a *side-contact* if and only if they have a full side in common. It is not allowed that a side is contained in more than two polygons. Notice that we do not require that all polygon sides are incident to two polygons. For brevity, we call representations of convex polygons in 3D with such side-contacts simply *side-contact representations* throughout the paper and every polygon will be considered as convex.

It is an open question to characterize the graphs that have a side-contact representation. First results were given by Arseneva et al. [2], who introduced this kind of contact representation. We list some of the results from Arseneva et al.: Exactly the planar graphs have a side-contact representation in the plane. The graph K_5 has no side-contact representation in 3D, but $K_{3,5}$ and $K_{4,4}$ have one. Another graph that has no side-contact representation is $K_{5,81}$, which implies by the Kővari–Sós–Turán theorem [5] that graphs with side-contact representation have at most $O(n^{9/5})$ edges, for n being the number of vertices. On the other

hand all graphs of hypercubes have a side-contact representation and thus there are n-vertex graphs with $\Theta(n \log n)$ edges with side-contact representation.

There exists a large body of literature for other types of contact representations. For a few selected results in 2D we redirect the reader to Arseneva et al. [2]. For 3D we list some selected results here: Due to Tietze [8] every graph has a contact representation with interior-disjoint convex polytopes in $\mathbb{R}^3$ where contacts are given by shared 2-dimensional facets. Evans et al. showed that every graph has a contact representation in 3D where two convex polygons touch if they share a single corner [3]. Every planar graph has a contact representation with axis-parallel cubes in $\mathbb{R}^3$ as shown by Felsner and Francis [4] (two cubes touch if their boundaries intersect), a similar result for boxes was discovered earlier by Thomassen [7]. Kleist and Rahman [6] studied a similar model but required that the intersection has nonzero area. They proved that every subgraph of an Archimedean grid can be represented with unit cubes. Alam et al. [1] showed in the same model with axis-aligned boxes that every 3-connected planar graph and its dual can be represented simultaneously.

Our contribution. We extend the results of Arseneva et al. [2] for complete bipartite graphs. We construct a side-contact representation of $K_{3,8}$, where previously only a construction for $K_{3,5}$ was known. On the other hand, we prove that $K_{3,250}$ has no side-contact representation. As a consequence the number of edges of an n-vertex graph with a side-contact representation is bounded by $O(n^{5/3})$.
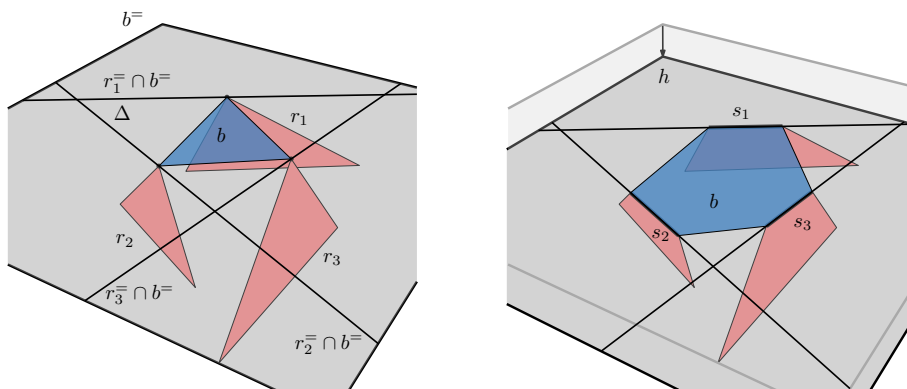
2   A side-contact representation for $K_{3,8}$

In this section we explain how to construct a side-contact representation of $K_{3,8}$. As an intermediate step we construct a *corner-contact representation*. In contrast to side-contact representations, two polygons touch with corner-contact if they share a single corner. For a polygon p its supporting plane $p^=$ defines two open half-spaces which we label arbitrarily as p^+ and p^-. We say that a representation (either corner-contact or side-contact) is *one-sided*, if for every polygon p its touching polygons lie either all in the closure of p^+, or they lie all in the closure of p^-. Note that the definition of one-sided is slightly stronger than the definition of *one-sided with respect to a set* as used by Arseneva et al. [2].

Lemma 1. *Every one-sided corner-contact representation of $K_{3,8}$ can be transformed into a side-contact representation of $K_{3,8}$.*

Proof. We call the polygons from the partition class with eight elements the blue polygons. Every blue polygon b can be trimmed to a triangle touching the (red) polygons r_1, r_2, r_3. We can assume for every b that the red polygons lie in $b^+ \cup b^=$. Consider the plane $b^=$ and the line arrangement $\mathcal{A}$ given by $b^= \cap r_i^=$ for $i \in \{1, 2, 3\}$. Since the representation is one-sided, $\mathcal{A}$ contains a triangular cell Δ such that every edge of Δ contains exactly one corner of b. Let h be a plane parallel to $b^=$ (inside b^+, very close to $b^=$) such that the line arrangement given by $h \cap r_i^=$ for $i \in \{1, 2, 3\}$ is combinatorially equivalent to $\mathcal{A}$ and furthermore the

cell corresponding to Δ contains on every edge exactly one line segment from $S = \{s_i := h \cap r_i \mid i \in \{1,2,3\}\}$. We can now replace b by the convex hull of S and then restrict the red polygons to $b^= \cup b^+$, w.r.t. the modified b. Since the three segments of S lie on the boundary of Δ, they all appear on its convex hull. Thus we keep all incidences without introducing new ones (see Figure 1). Also, the one-sidedness property is maintained. Repeating this for every blue polygon yields a side-contact representation of $K_{3,8}$.


Fig. 1. Offsetting the supporting planes of the blue polygons can transform a one-sided corner-contact representation into a side-contact representation.

It remains to construct a one-sided corner-contact representation for $K_{3,8}$. We start with a hexagonal prism of height 1. Its base is parallel to the xy-plane and given by a hexagon with alternating side lengths 2 and 14 and interior angles of $2\pi/3$. We name the corners of the bottom base (in cyclic order) $x_0, \ldots, x_5$, and the corners at the top $x'_0, \ldots, x'_5$, such that x_i and x'_i are adjacent. All indices of these points are considered modulo 6. Let ℓ_i be the segment between x_{2i+1} and x'_{2i+4} for $i \in \{1,2,3\}$. For any ℓ_i we define ℓ'_i to be a copy of ℓ_i that is vertically shifted up by 0.2. Now, we subdivide all six segments in the middle and move the subdivision point vertically up by 1.08 in case of the ℓ'_is and vertically down by 1.08 in case of the ℓ_is. We define for all $i \in \{1,2,3\}$ the (red) polygon r_i as the convex hull of ℓ_i and ℓ'_i (including the translated subdivision point). Notice that the polygons are disjoint (see appendix). The convex hull of these polygons defines a convex polyhedron $\mathcal{P}$. We observe that $\mathcal{P}$ has eight triangular faces that are incident to all red polygons. These define the blue polygons (see Figure 2). Note that at the subdivision points we have one red polygon adjacent to two blue polygons. To resolve this issue we replace all subdivision points by an ε-small side such that the red polygons remain convex and all blue polygons still appear on the convex hull of $\{r_1, r_2, r_3\}$ (details are given in the appendix). We then move the corners of the adjacent blue polygons to two distinct endpoints of the new sides. It can be checked (see also appendix) that the constructed

representation is one-sided (in particular, the red polygons are contained in $\mathcal{P}$) and therefore, by Lemma 1 it can be transformed into a (one-sided) side-contact representation. We summarize our result.

Theorem 1. *The graph $K_{3,8}$ has a side-contact representation with convex polygons in 3D.*
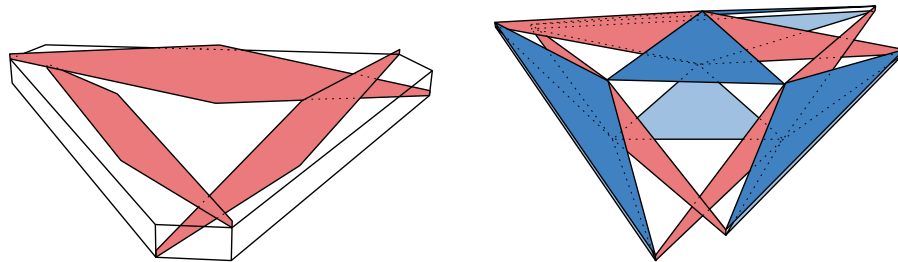
Fig. 2. The configuration of the red polygons and the prism (left). The full configuration (right).

We remark that the side-contact representation of $K_{3,8}$ is one-sided. As a consequence of a result by Arseneva et al. [2, Lemma 11] no $K_{3,t}$ with $t > 8$ has a one-sided representation with side-contacts.

3 $K_{3,250}$ has no side-contact representation

In this section we prove the following result:

Theorem 2. *The graph $K_{3,250}$ has no side-contact representation with convex polygons in 3D.*

To prove Theorem 2 we present first some lemmas for configurations of (straight-line) segments in 2D. Thus, until mentioned otherwise, all configurations are considered in 2D from now on. We say that a set of segments $\mathcal{S}$ is convex if every $s \in \mathcal{S}$ lies on the convex hull of $\mathcal{S}$ and no two segments have the same slope. We allow that in a convex set of segments two segments share an endpoint. Assume that the elements of $\mathcal{S}$ are named such that the sequence $s_1, s_2 \ldots, s_m$ lists the segments according to their clockwise appearance on the convex hull. The intersection of the supporting lines of two segments s_i and s_j is called *support intersection point* (si-point for shorthand notation) of s_i and s_j. If $j = i + 1$, or $i = 1$ and $j = m$, we call the si-point of s_i and s_j a *consecutive support intersection point* (csi-point for shorthand notation). Let $s_i = a_i b_i$ and $s_j = a_j b_j$ such that $a_i b_j$ is a proper segment on the convex hull of $\mathcal{S}$. The csi-point c_{ij} of s_i and s_j is called *flopped* if the line through $a_i b_j$ defines a closed half-space that contains c_{ij} and $\mathcal{S}$. See Figure 3 for an illustration.
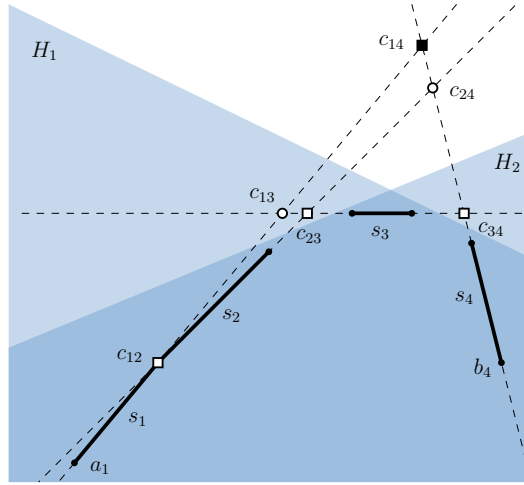
Fig. 3. Four segments in convex position. Csi-points are shown as squares. The only flopped csi-point c_{14} is filled. All other si-points are drawn as (empty) disks.

Lemma 2. *For any set $\mathcal{S}$ of segments in convex positions there is at most one csi-point that is flopped.*

Proof. Let s_i and s_j be two segments with csi-point c_{ij}. We can assume that $j = i + 1$. The point c_{ij} can only be flopped if the clockwise radial sweep of the tangent lines from s_i to s_j requires an angle larger than π, since we need to transition a state in which the tangent line is parallel to s_i. Since in a total angular sweep we rotate by 2π, this can happen only once.

Lemma 3. *Let $\mathcal{S}$ be a set of at least four segments in convex position. Consider any two closed half-spaces H_1 and H_2 that (i) both contain $\mathcal{S}$, and (ii) no $s \in \mathcal{S}$ is completely part of the boundary of H_1 or H_2. Then at least one csi-point of S lies in the interior of $H_1 \cap H_2$.*

Proof. Assume first that $\mathcal{S}$ contains no flopped csi-point. Then the set of csi-points forms a convex set C. Furthermore, every edge of the convex hull of C contains exactly one segment of $\mathcal{S}$ completely. Consider now a closed half-space H that contains $\mathcal{S}$. If the interior of H misses two points from C, then an edge of the convex hull of C (and therefore a segment of $\mathcal{S}$) lies in the complement of the interior of H. Clearly H violates condition (i) or (ii) from the statement of the lemma in this case.

Now assume that we have a flopped csi-point c. We can augment $\mathcal{S}$ by adding a new segment such that the new set is convex and has no flopped csi-point. All csi-points other than c will remain. Thus, also in this situation, at most one nonflopped csi-point is not in the interior of H if the boundary of H contains no segment from $\mathcal{S}$ completely.

The interior of the intersection of any two closed half-spaces H_1 and H_2 fulfilling (i) and (ii) can therefore miss no more than one nonflopped csi-point per half-space, and possibly a flopped csi-point if it exists. By Lemma 2 there can only be one flopped csi-point. The statement of the lemma follows.

We remark that the statement of Lemma 3 is "tight" as shown by the configuration in Figure 3.

Lemma 4. *Let $\mathcal{S} = \{s_1, \ldots, s_m\}$ be a set of segments in convex position indexed in cyclic order. Assume that $s_1 = aa'$ and $s_m = bb'$ define a flopped csi-point c such that the segment ab lies on the convex hull of $\mathcal{S}$. Then all si-points of $\mathcal{S}$ lie inside the triangle Δ spanned by a, b and c.*

Proof. Let ℓ_i be the supporting line of s_i. We denote the intersection of ℓ_i with ℓ_j by x_{ij}. Notice that on ℓ_1 the following points appear in order: $a, x_{12}, x_{13}, \ldots, x_{1m}, c$. On ℓ_m however, we have the order: $b, x_{m(m-1)}, \ldots, x_{m2}, x_{m1}, c$. Both facts can be observed by radially sweeping a tangent line around the convex hull of $\mathcal{S}$.

Now consider any two segments $s_i, s_j \in \mathcal{S}$, with $1 < i < j < m$. Their si-point is denoted as x_{ij}. Since on ac the order of points is a, x_{1i}, x_{1j}, c and on bc the order of points is b, x_{mj}, x_{mi}, c the segments $x_{1i}x_{mi}$ and $x_{1j}x_{mj}$ have to cross inside Δ and hence the si-point defined by s_i and s_j lies in Δ (see also Figure 4). We have already observed that all other relevant si-points (defined by either s_1 or s_m) lie on the boundary of Δ.
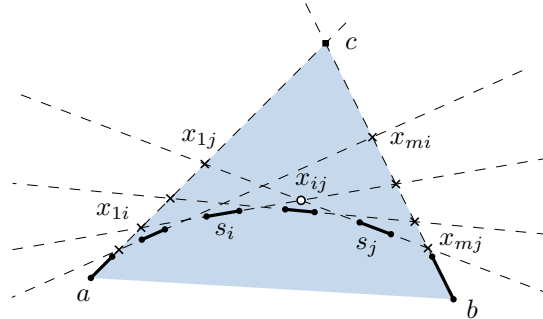
Fig. 4. Illustration of the proof of Lemma 3. The triangle Δ is shaded blue and the si-point induced by s_i and s_j is drawn as empty disk.

We now prove Theorem 2 and go back to 3D.

Proof. (Theorem 2). Assume that we have a side-contact representation of $K_{3,250}$. We call the polygons r_1, r_2, r_3 of the first partition class the *red polygons*. The polygons of the other partition class are called the *blue polygons*. The supporting plane of a polygon r_i is named $r_i^=$. Let $\mathcal{A}$ be the arrangement given by $r_1^=, r_2^=, r_3^=$. We can assume that the three planes intersect in a single point r_*, and that no

two sides of a polygon are parallel. Otherwise we apply suitable (small) projective transformations to prevent parallel planes and lines without disconnecting the polygons. We call the eight (closed) cells of $\mathcal{A}$ *octants*. Note that every blue polygon has to lie in a single octant, since it has a side-contact with each of the red polygons. A red polygon can only be part of all octants if it contains r_*. Thus, at least two red polygons need to avoid r_* and "miss" at least two octants each, and only one of these octants can be the same. As a consequence there are at most 5 octants that have a piece of every red polygon on the boundary. One of them contains at least $50 = 250/5$ blue polygons. We denote this octant by $\mathcal{C}$.

Let f_i be the bounding face of $\mathcal{C}$ that contains r_i and denote the interior of f_i by $\tilde{f}_i$. Further let ρ_{ij} be $f_i \cap f_j$. Both r_1 and r_2, can have at most one side fully contained in ρ_{12} and no side from r_3 can be completely in ρ_{12} since $\rho_{12} \cap r_3^{=} = \{r_*\}$. Thus, $\rho := \rho_{12} \cup \rho_{23} \cup \rho_{13}$ contains at most six complete sides from blue polygons in $\mathcal{C}$. We ignore any blue polygon with a full side in ρ and remain with a set B of at least 44 blue polygons.

First, we consider the polygon r_1 and select a set $\mathcal{S}_1$ of 44 of its sides that are incident to some polygon in B. As usual, we label the segments $s_1, s_2, \ldots, s_{44}$ cyclically and set $\mathcal{S}_1' = \{s_1, s_{12}, s_{23}, s_{34}\}$. The face f_1 can be obtained by intersecting $r_1^{=}$ with two closed half-spaces. No segments of $\mathcal{S}_1'$ lies completely on the boundary of f_1 and thus, by Lemma 3 at least one csi-point, say c, of $\mathcal{S}_1'$ lies in $\tilde{f}_1$. Take the two segments aa' and bb' (with $a'b'$ on the convex hull on $\mathcal{S}_1'$) defining c and all of the ten segments of $\mathcal{S}$ in between them in the cyclic order. We call this set $\mathcal{S}_1''$. Note that this set has a flopped csi-point, which is c. Since a, b, c lie in $\tilde{f}_1$ we have by Lemma 4 that all si-points of $\mathcal{S}_1''$ lie in $\tilde{f}_1$.

We now deal with polygon r_2. Let $\mathcal{S}_2$ be the set of sides of r_2 that share a side with a blue polygon that has a side in $\mathcal{S}_1''$. We get that $|\mathcal{S}_2| = 12$. We sort the segments in $\mathcal{S}_2$ again by a radial sweep (notice that the order might be different than in $\mathcal{S}_1''$). This time we select the first, fourth, seventh and tenth segment in this order and we denote this subset by $\mathcal{S}_2'$. Again, we apply Lemma 3 to find a csi-point in $\tilde{f}_2$ and then Lemma 4 to obtain a set $\mathcal{S}_2''$ of (this time 4) segments, whose si-points are all in $\tilde{f}_2$.

Finally, we consider r_3. Let $\mathcal{S}_3$ be the set of sides of r_3 that share a side with a blue polygon that has a side in $\mathcal{S}_2''$ (and therefore in $\mathcal{S}_1''$ as well). Since $|\mathcal{S}_2| = 4$ we get by Lemma 3 that one csi-point of $\mathcal{S}_3$ lies in $\tilde{f}_3$. Two segments of $\mathcal{S}_3$ define this point. Call the adjacent blue polygons b_1 and b_2, with supporting planes $b_1^{=}$ and $b_2^{=}$. We denote the restriction of $b_1^{=}/b_2^{=}$ to the boundary of $\mathcal{C}$ by t_1/t_2. By our construction, t_1 and t_2 intersect on $\tilde{f}_3$ in a csi-point. But both blue polygons have also a common side with each of the sets $\mathcal{S}_2''$ and $\mathcal{S}_1''$. As a consequence, t_1 and t_2 intersect in an si-point of $\mathcal{S}_1''$ inside $\tilde{f}_1$ and in an si-point of $\mathcal{S}_2''$ inside $\tilde{f}_2$. The three si-points are distinct and define a plane. We get that $b_1^{=} = b_2^{=}$. However, if two blue polygons lie in the same plane, all red polygons and therefore all blue polygons have to lie in this plane as well. Since $K_{3,250}$ is nonplanar, it has no side-contact representation in the plane, and we have obtained the desired contradiction.

The following is now a simple consequence from the Kővari–Sós–Turán theorem [5], which states that an n-vertex graph that has no $K_{s,t}$ as a subgraph can have at most $O(n^{2-1/s})$ edges.

Corollary 1. *Let G be an n-vertex graph with a side-contact representation of convex polygons in 3D. Then the number of edges in G is bounded by $O(n^{5/3})$.*

References

1. Md. Jawaherul Alam, William Evans, Stephen G. Kobourov, Sergey Pupyrev, Jackson Toeniskoetter, and Torsten Ueckerdt. Contact representations of graphs in 3D. In Frank Dehne, Jörg-Rüdiger Sack, and Ulrike Stege, editors, *Proc. Algorithms and Data Structures Symposium (WADS'15)*, volume 9214 of *LNCS*, pages 14–27, 2015.
2. Elena Arseneva, Linda Kleist, Boris Klemz, Maarten Löffler, André Schulz, Birgit Vogtenhuber, and Alexander Wolff. Adjacency graphs of polyhedral surfaces. In Kevin Buchin and Éric Colin de Verdière, editors, *Proc. 37th International Symposium on Computational Geometry (SoCG '21)*, volume 189 of *LIPIcs*, pages 11:1–11:17. Schloss Dagstuhl - Leibniz-Zentrum für Informatik, 2021. full version https://arxiv.org/abs/2103.09803v2.
3. William Evans, Paweł Rzazewski, Noushin Saeedi, Chan-Su Shin, and Alexander Wolff. Representing graphs and hypergraphs by touching polygons in 3D. In Daniel Archambault and Csaba Tóth, editors, *Proc. Graph Drawing & Network Vis. (GD'19)*, volume 11904 of *LNCS*, pages 18–32. Springer, 2019.
4. Stefan Felsner and Mathew C. Francis. Contact representations of planar graphs with cubes. In Ferran Hurtado and Marc J. van Kreveld, editors, *Proc. 27th Ann. Symp. Comput. Geom. (SoCG'11)*, pages 315–320. ACM, 2011.
5. Tamás Kővari, Vera T. Sós, and Pál Turán. On a problem of K. Zarankiewicz. *Coll. Math.*, 3(1):50–57, 1954.
6. Linda Kleist and Benjamin Rahman. Unit contact representations of grid subgraphs with regular polytopes in 2D and 3D. In Christian Duncan and Antonios Symvonis, editors, *Proc. Graph Drawing (GD'14)*, volume 8871 of *LNCS*, pages 137–148. Springer, 2014.
7. Carsten Thomassen. Interval representations of planar graphs. *J. Combin. Theory Ser. B*, 40(1):9–20, 1986.
8. Heinrich Tietze. Über das Problem der Nachbargebiete im Raum. *Monatshefte für Mathematik und Physik*, 16(1):211–216, 1905.

A   Omitted Details for the Construction in Section 2

We give here the full details how to obtain the one-sided corner-contact representation of $K_{3,8}$. We start with the precise definitions of the coordinates. Let $q_1, \ldots, q_8$ be the points of the first red polygon r_1. For a point $q \in \mathbb{R}^3$ we denote its coordinates by (q^x, q^y, q^z). The coordinates for r_1 are chosen as follows

i	1	2	3	4	5	6	7	8
q_i^x	8	8	0.08	0	-8	-8	-0.08	0
q_i^y	$2\sqrt{3}$	$2\sqrt{3}$	$2\sqrt{3}$	$2\sqrt{3}$	$2\sqrt{3}$	$2\sqrt{3}$	$2\sqrt{3}$	$2\sqrt{3}$
q_i^z	-0.6	-0.4	1.1815	1.1814	0.6	0.4	-1.1815	-1.1814
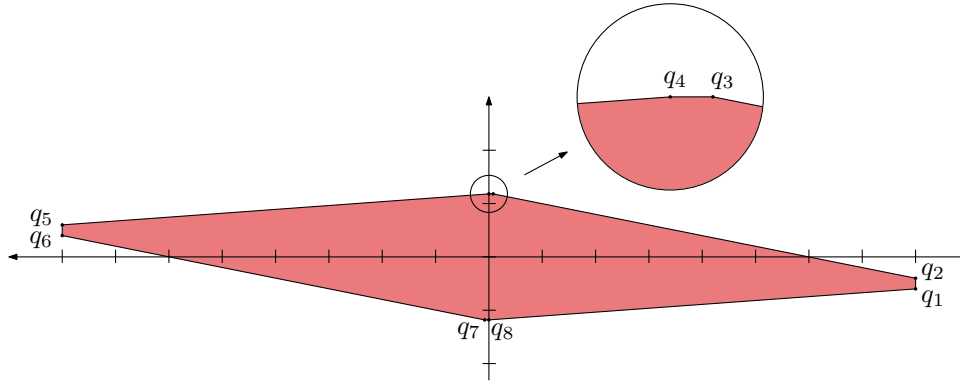
Fig. 5. The shape of a red polygon.

The red polygon r_2 is obtained by rotating a copy r_1 around the z-axis by $2\pi/3$. Similarly, r_3 is given by a copy of r_1 rotated by $-2\pi/3$ around the z-axis. We denote the vertices of r_2 by $s_1, \ldots, s_8$ and the vertices of r_3 by $t_1, \ldots, t_8$, such that s_i/t_i are copies of q_i. We need to assure that the three polygons are disjoint. When looking at the top view (Figure 6) we see that there can be at most three possible intersections, marked with a cross in the figure. Due to symmetry we only need to check one of these locations. Thus, it suffices to assure that segment q_2q_3 lies below segment t_6t_7 at the line v parallel to the z-axis through the point x, where $x = (6, 2\sqrt{3}, 0)$ is the intersection of r_1 and r_3 when projected into the xy-plane. Computing the distances shows that the z-coordinate of $q_2q_3 \cap v$ is -0.000631313 and therefore negative. By symmetry $t_6t_7 \cap v$ has a positive z-coordinate and hence the two red polygons are disjoint.

Fig. 6. Top view of the representation.

To specify a blue polygon b, we write $b = (q_i, s_j, t_k)$ if the corners of b are q_i, s_j, t_k. The blue polygons are then given as follows:

$$b_1 = (q_4, s_5, t_2) \qquad b_2 = (q_8, s_6, t_1) \qquad b_3 = (q_2, s_4, t_5) \qquad b_4 = (q_1, s_8, t_6)$$
$$b_5 = (q_5, s_2, t_4) \qquad b_6 = (q_6, s_1, t_8) \qquad b_7 = (q_3, s_3, t_3) \qquad b_7 = (q_7, s_7, t_7)$$

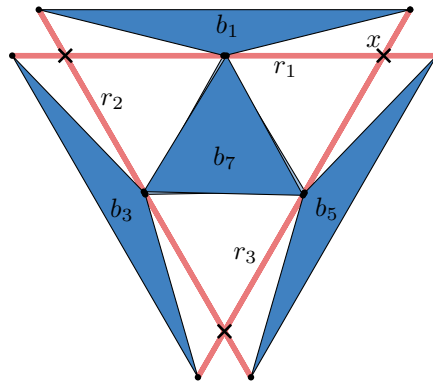It remains to check if the configuration of red and blue polygons is one-sided. To decide for a polygon p on which side of the supporting plane $p^=$ a point q lies we can use the signed volume of the tetrahedron spanned by q, q_1, q_2, q_3, where q_1, q_2, q_3 are three arbitrary corners of p. This volume can be computed with the following expression:

$$[q, q_1, q_2, q_3] := \det \begin{pmatrix} q^x & q_1^x & q_2^x & q_3^x \\ q^y & q_1^y & q_2^y & q_3^y \\ q^z & q_1^z & q_2^z & q_3^z \\ 1 & 1 & 1 & 1 \end{pmatrix}$$

Thus, for every polygon p' adjacent to p we have to check if the nonzero entries of $\{[q', q_1, q_2, q_3] \mid q' \text{ is corner of } p'\}$ have all the same sign. We finish with a small python-3 script that will carry out the necessary computations. Running the script verifies that the configuration is a one-sided corner-contact representation of $K_{3,8}$.

```python
import numpy as np
import math

def check_side(pa,polygonlist):
    """ Processes all polygons in polygonlist
    Prints "true" if all polygons in polygonlist are on
    one side of polygon pa.
    """
    for pb in polygonlist:
        orientation = []
        for point in pb:
            m1 = np.array([pa[0],pa[1],pa[2],point])
            m2 = np.insert(m1,3,[1,1,1,1],1)
            orientation.append(np.linalg.det(m2))
        a = np.array(orientation)
        print(np.any((a <= 0)|(a >= 0 )))


red2d = np.array([[8,-.6],[8,-.4],[.08,1.1815],[0,1.1814],[-8,.6],
        [-8,.4],[-.08,-1.1815],[0,-1.1814]],)
red1 = np.insert(red2d,1,np.full((1,8),2*math.sqrt(3)),1)
rot_matrix = np.array([[-1/2,-math.sqrt(3)/2,0],
        [math.sqrt(3)/2,-1/2,0],[0,0,1]])
```

```python
red2 = np.matmul(red1,rot_matrix)
red3 = np.matmul(red2,rot_matrix)

blue1 = np.array([red1[3],red2[4],red3[1]])
blue2 = np.array([red1[7],red2[5],red3[0]])
blue3 = np.array([red2[3],red3[4],red1[1]])
blue4 = np.array([red2[7],red3[5],red1[0]])
blue5 = np.array([red3[3],red1[4],red2[1]])
blue6 = np.array([red3[7],red1[5],red2[0]])
blue7 = np.array([red1[2],red2[2],red3[2]])
blue8 = np.array([red1[6],red2[6],red3[6]])

reds = [red1,red2,red3]
blues = [blue1,blue2,blue3,blue4,blue5,blue6,blue7,blue8]

for red in reds:
    check_side(red,blues)

for blue in blues:
    check_side(blue,reds)
```